Electronic Supplementary Material (ESI) for Chemical Communications
This journal is © The Royal Society of Chemistry 2012

Supporting information

Cooperative nucleophilic-electrophilic organocatalysis by ionic liquids

Vittorio Lucchini,* Marco Noè, Maurizio Selva, Massimo Fabris, Alvise Perosa*

Experimental procedures.

The reaction conditions. The experimental procedure for kinetic determination via ^{13}C NMR spectroscopy has already been described (reference 9 in the article). We here point to some differences. The desired quantities of the ionic liquid, or of DBU, or of phosphazene were weighed in a screw-cap NMR tube, which was charged with the correct volume of cyclohexenone. The tube was then equipped with a sealed capillary, containing pure [D_6]DMSO and blocked in a coaxial position by means of a Teflon spacer, for locking and homogeneity purposes. The kinetic measurements were directly run in the spectrometer, at the temperature of 60° C, as regulated by the spectrometer.
The course of a reaction, in the absence of a solvent, when reagents and products are at the greatest concentration, could be adequately followed by ^{13}C NMR spectroscopy. The spectra were collected under the regime of ^{1}H inverse gated decoupling, with the aim of minimizing NOE effects. In a typical experiment, a series of spectra were consecutively acquired: 16 or 32 scans per spectrum, 16 s relaxation delay, 32K of data points, FT with zero filling to 256K, Gaussian window function. The transformed spectra were subjected to automatic phase adjustment and line base correction. The signals selected as representative of the involved species were extracted and, in order to overcome the limits of the numerical integration procedure of the spectrometer, deconvoluted into a combination of Gaussian and Lorentzian functions:

alpha*Lorentzian + (1 - alpha)*Gaussian

and the analytical integral of this combination was evaluated. Examples of this procedure are presented, in a graphic form, in Figures S1-S5. The kinetic times were given by the internal clock of the spectrometer host computer.

The evaluation of the kinetic parameters. The kinetic times and the analytical integrals were then transferred into a Cartesian plot. The integrals required a normalization factor. Because no side reaction was observed, the sum of the integral representing cyclohexanone **7** and of twice the integral representing the dimer **8** was chosen as the normalization factor. Thus the normalized amounts of the species **7** and **8** were represented as “unitary molar fractions”, and symbolized by {**X**}. The amounts of the catalysts were similarly derived from their normalized integrals, properly weighed.
The most appropriate kinetic parameter that could offer a quantitative measure of the complex reaction system, represented by the scheme in the article, was the initial rate constant $-(d\{\mathbf{7}\}_0/dt)/\{\mathbf{7}\}_0$ for the decrease of cyclohexenone **7**. The initial rate $d\{\mathbf{7}\}_0/dt$ is customarily derived from the slope of the straight line passing through the first kinetic points. As the choice of the number of initial points is rather arbitrary, we devised to take advantage of the Newton interpolation of the whole set of kinetic points. A 5th degree polynomial was visually satisfactory. The first order coefficient $\mathbf{a_1}$ of the polynomial is the zero order coefficient of the derivative, and is the only surviving coefficient at zero time. As the attainment of the experiment

This journal is © The Royal Society of Chemistry 2012

temperature and of a satisfactory homogeneity was not instantaneous, the very initial kinetic points were usually missed, and the value of $\{\mathbf{7}\}_0$ was less than unitary. The determination of $\{\mathbf{7}\}_0$ rested upon a single measurement: a better choice was the intercept of the polynomial $\mathbf{a_0}$. Thus the ratio $-\mathbf{a_1}/\mathbf{a_0}$ could be considered the best estimation for $-(d\{\mathbf{7}\}_0/dt)/\{\mathbf{7}\}_0$.
The results for the "productive" kinetic runs are presented in Figures S6-S15. It can be appreciated that the molar fractions of the catalysts did non change during the whole reaction course. The average values are reported in the article table. Because of the elevated number of monitored points, the errors on the values of $\mathbf{a_1}$ and $\mathbf{a_0}$ and on the average catalyst molar fractions are negligible.

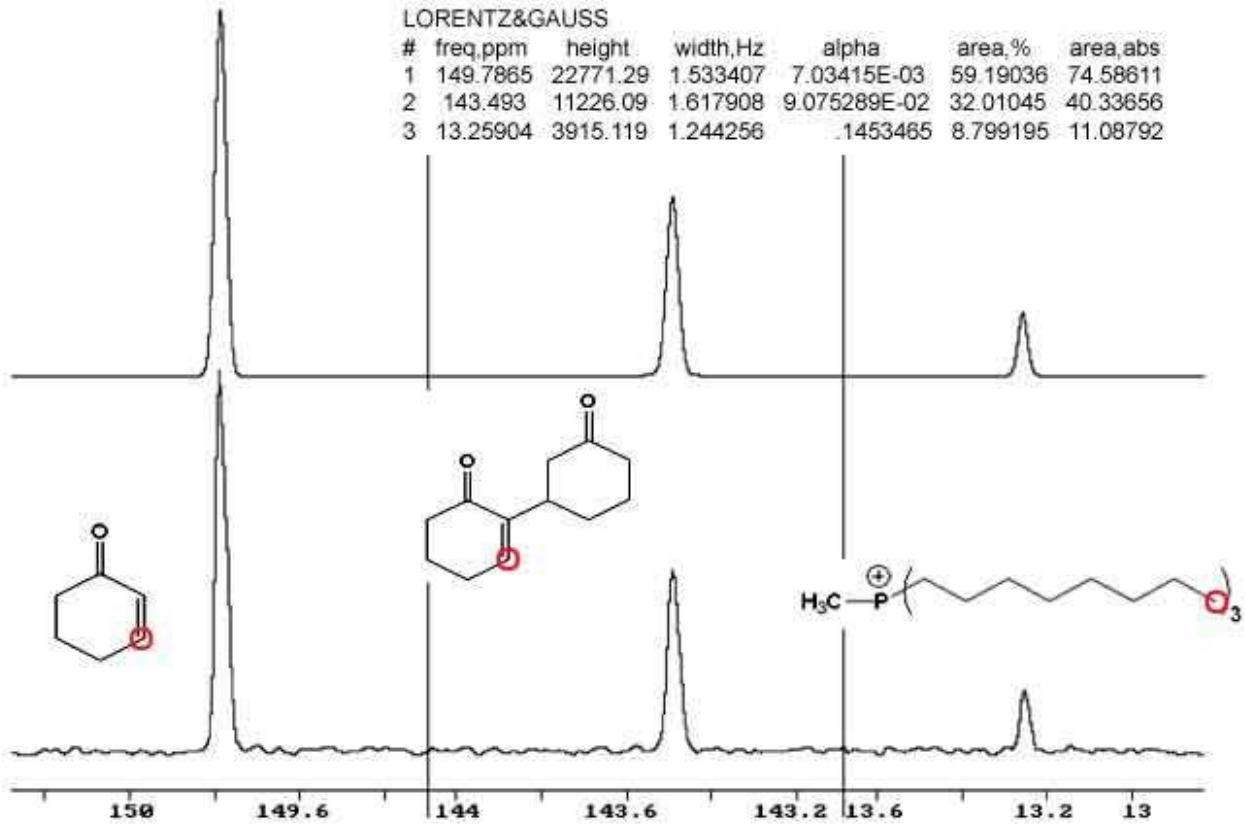

Figure S1. Example of deconvolution of selected ^{13}C resonances for the evaluation of the kinetic runs 1 and 2 in Scheme 1. Taken from run 1, spectrum monitored at time 1.69 h.

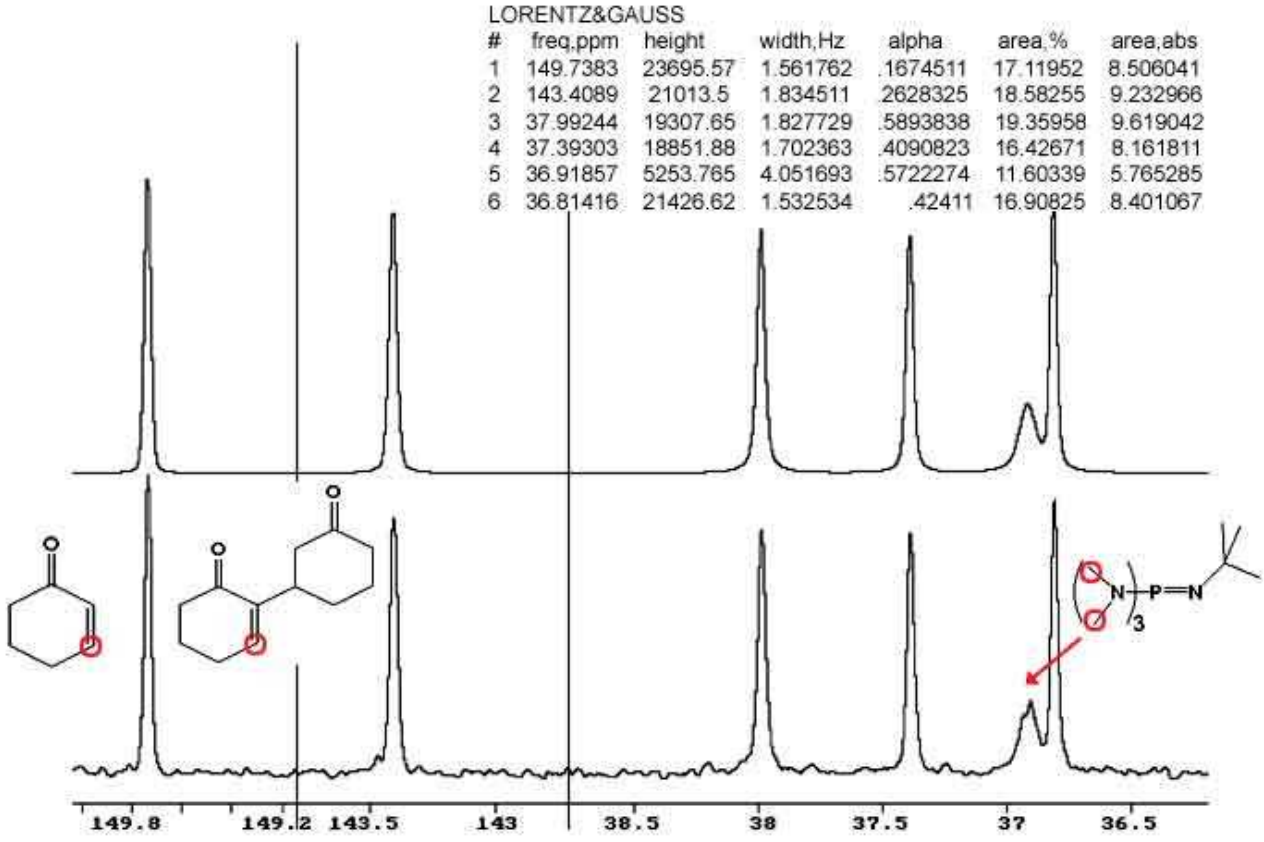

Figure S2. Example of deconvolution of selected ^{13}C resonances for the evaluation of the kinetic run 5 in Scheme 1. Taken from spectrum monitored at time 3.70 h.

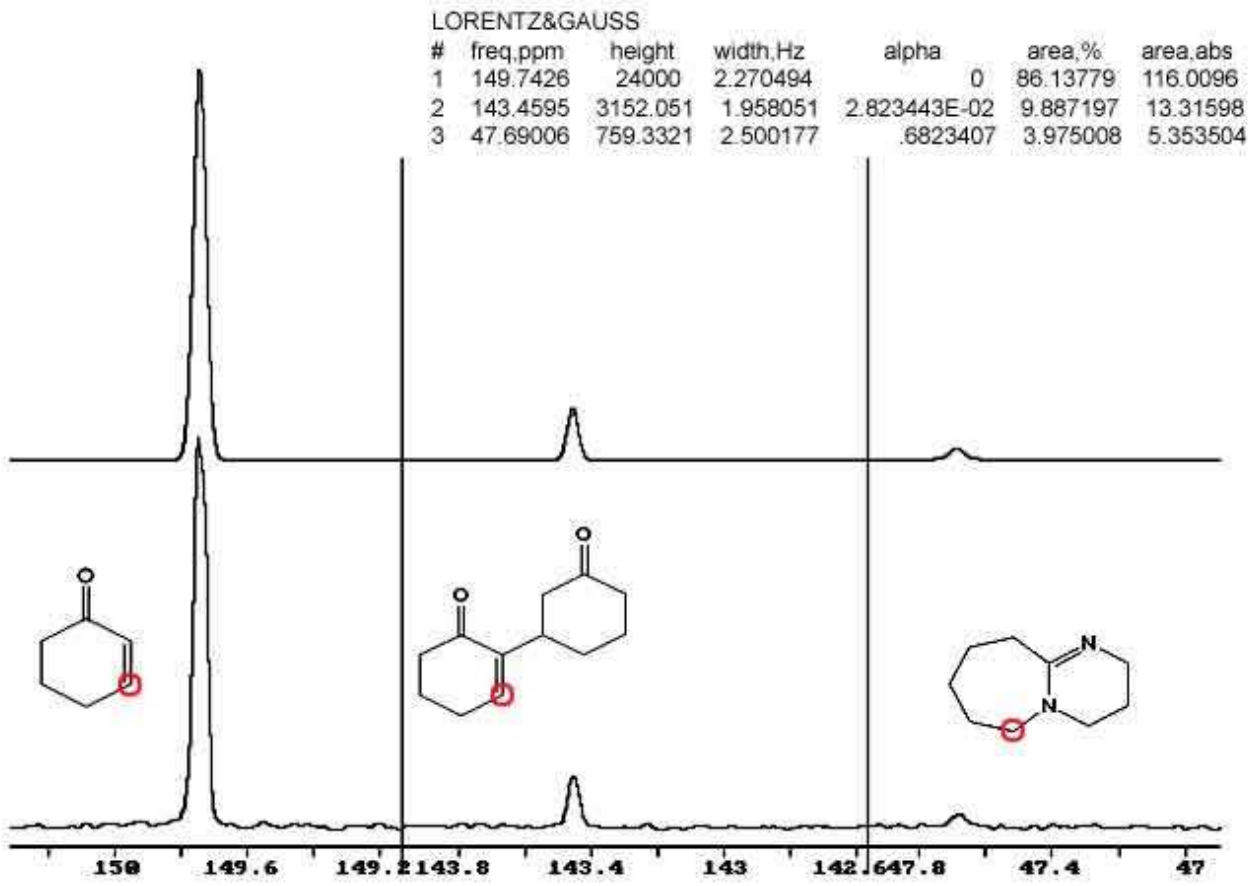

Figure S3. Example of deconvolution of selected ^{13}C resonances for the evaluation of the kinetic run 6 in Scheme 1. Taken from spectrum monitored at time 3.48 h.

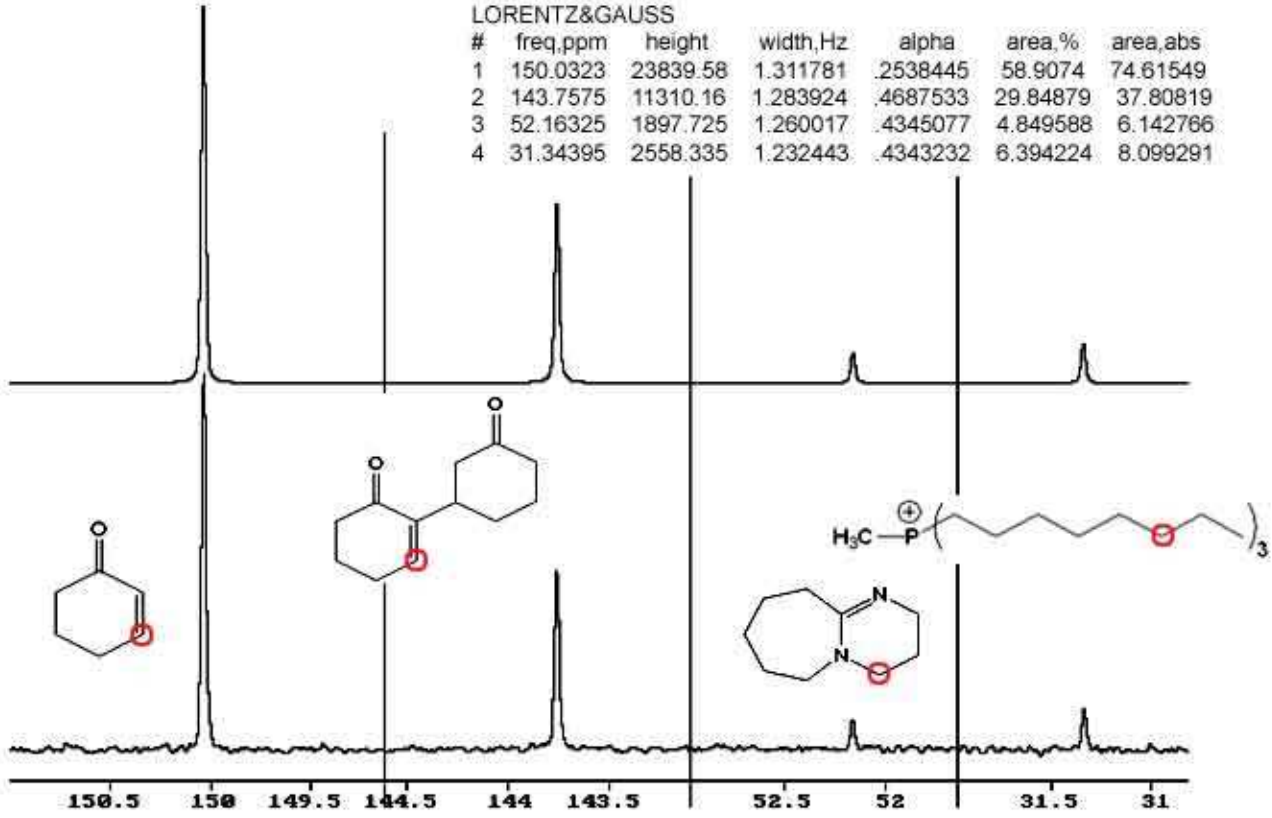

Figure S4. Example of deconvolution of selected ^{13}C resonances for the evaluation of the kinetic runs 7-11 in Scheme 1. Taken from run 9, spectrum monitored at time 2.93 h.

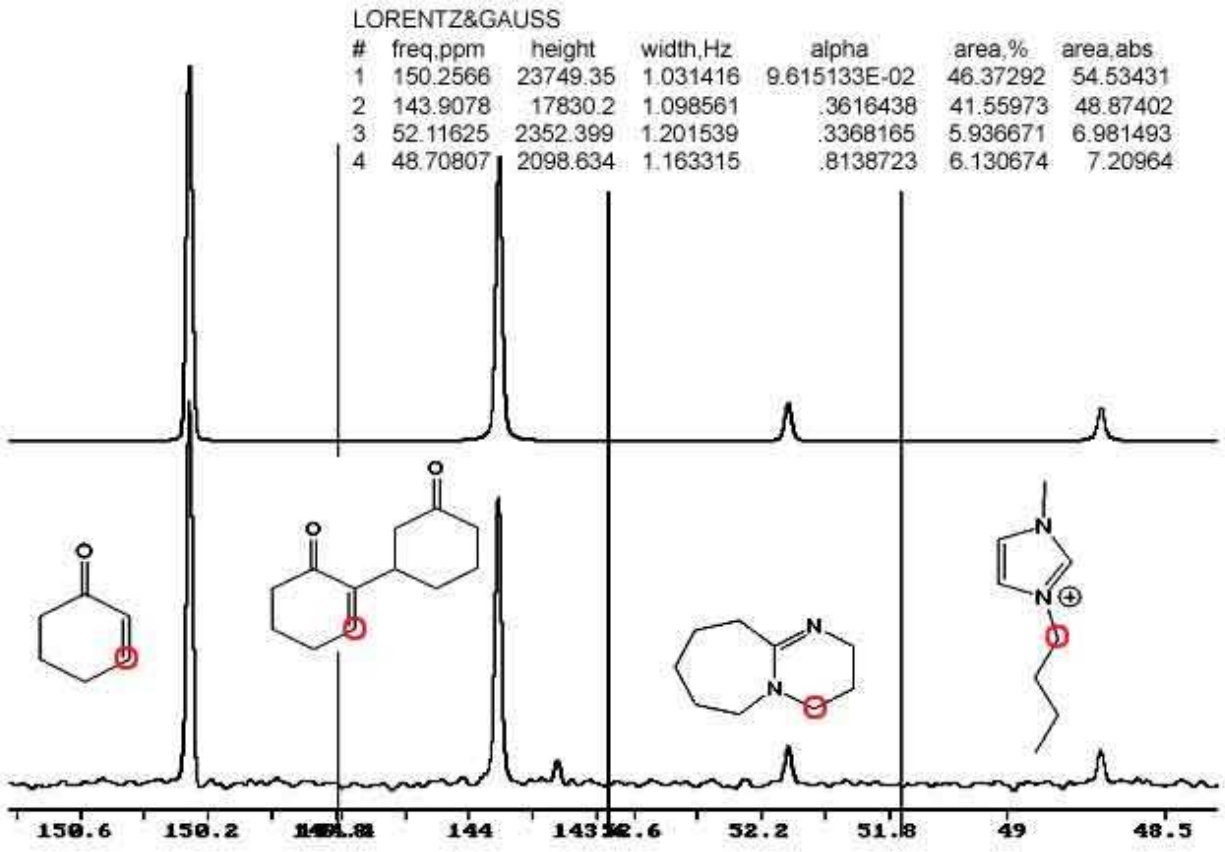

Figure S5. Example of deconvolution of selected ^{13}C resonances for the evaluation of the kinetic run 12 in Scheme 1. Taken from spectrum monitored at time 1.69 h.

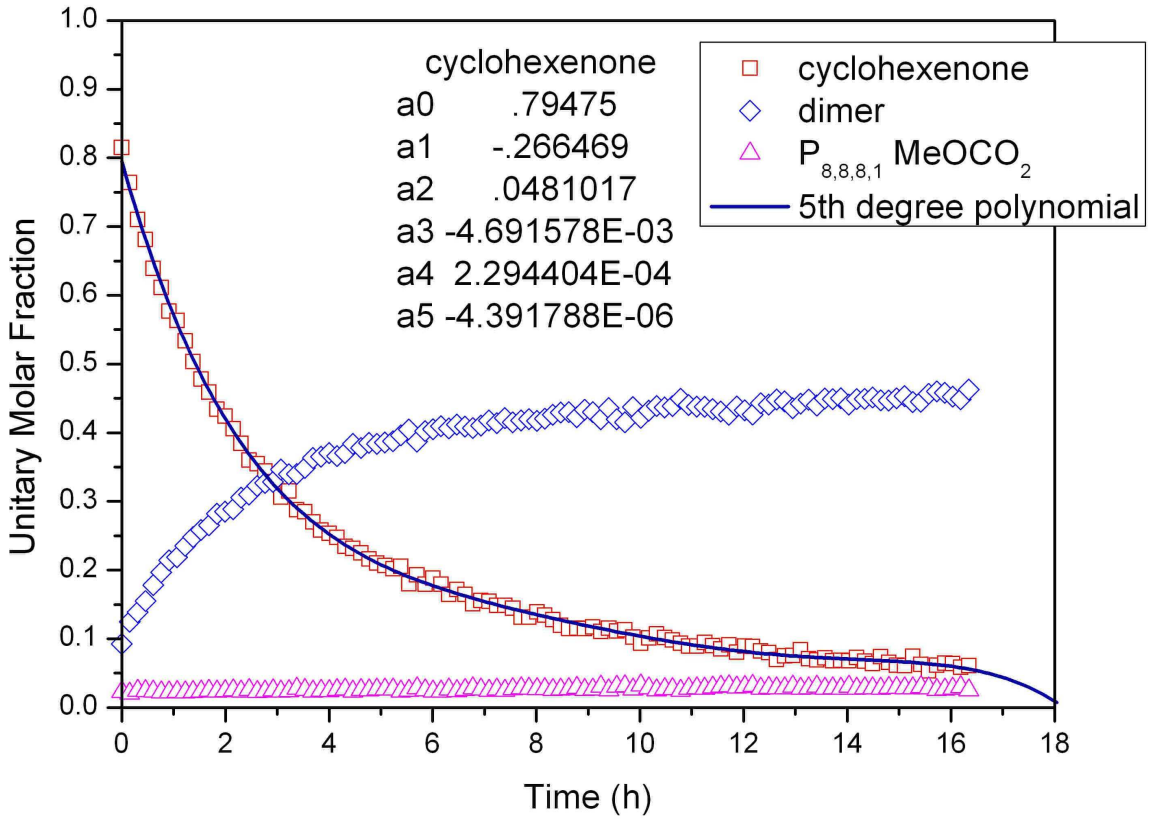

Figure S6. Conversion (entry 1 in the table) of cyclohexenone **7** into dimer **8** under the catalysis of $P_{8,8,8,1}$ $MeOCO_2$ **1**. The interpolation of the decrese of **7** into a 5th degree polynomial and the corresponding coefficients are shown.

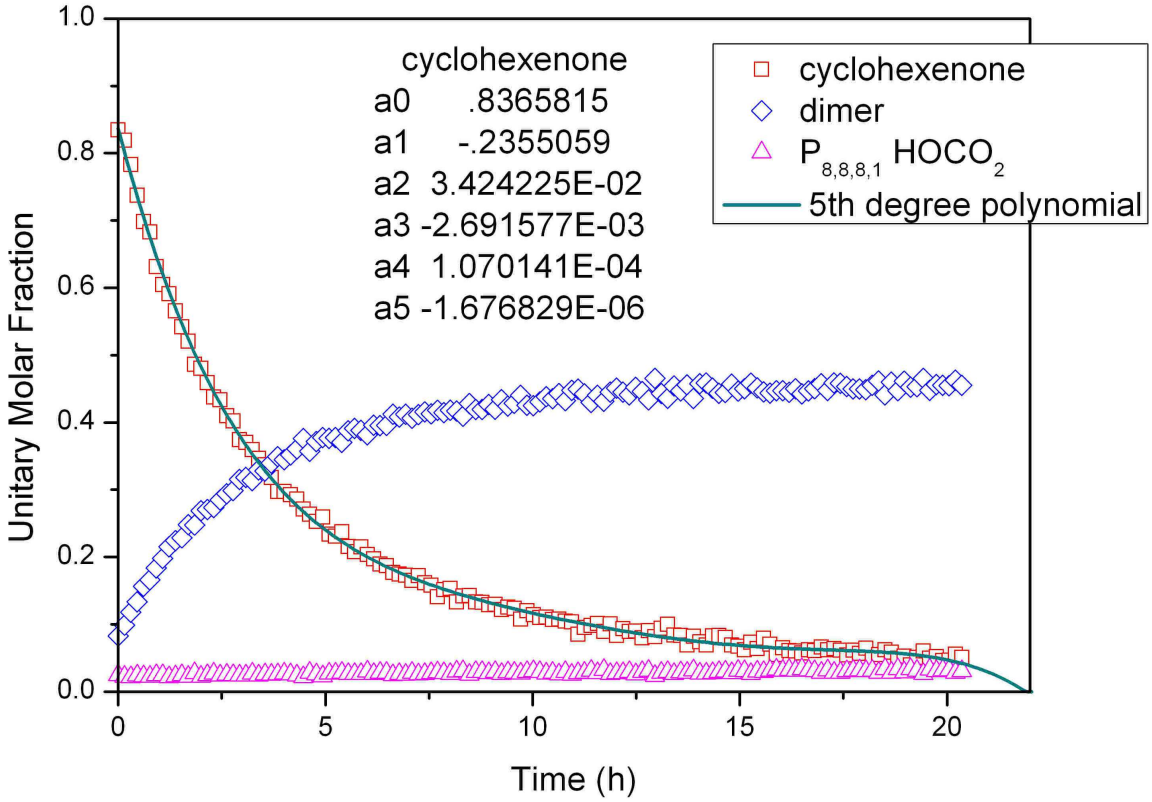

Figure S7. Conversion (entry 2 in the table) of cyclohexenone **7** into dimer **8** under the catalysis of $P_{8,8,8,1}$ $HOCO_2$ **2**. The rest of the caption as in Figure S6.

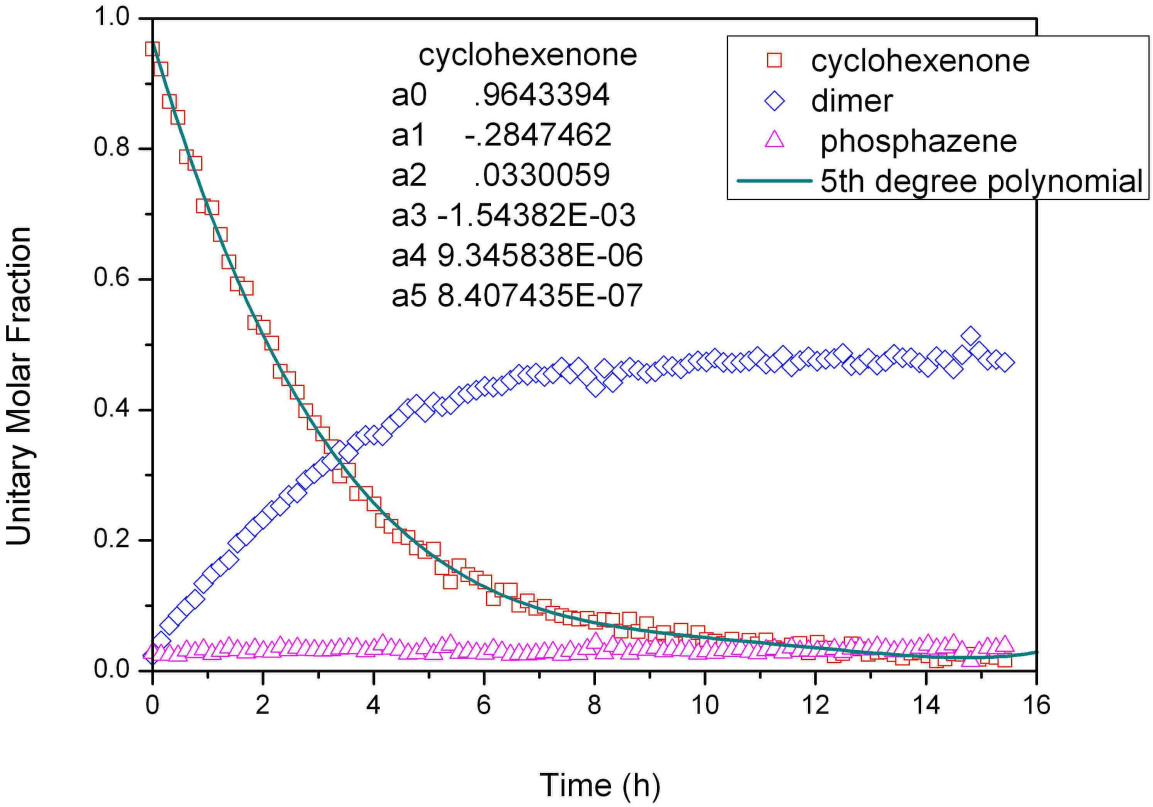

Figure S8. Conversion (entry 5 in the table) of cyclohexenone **7** into dimer **8** under the catalysis of phosphazene **5**. The rest of the caption as in Figure S6.

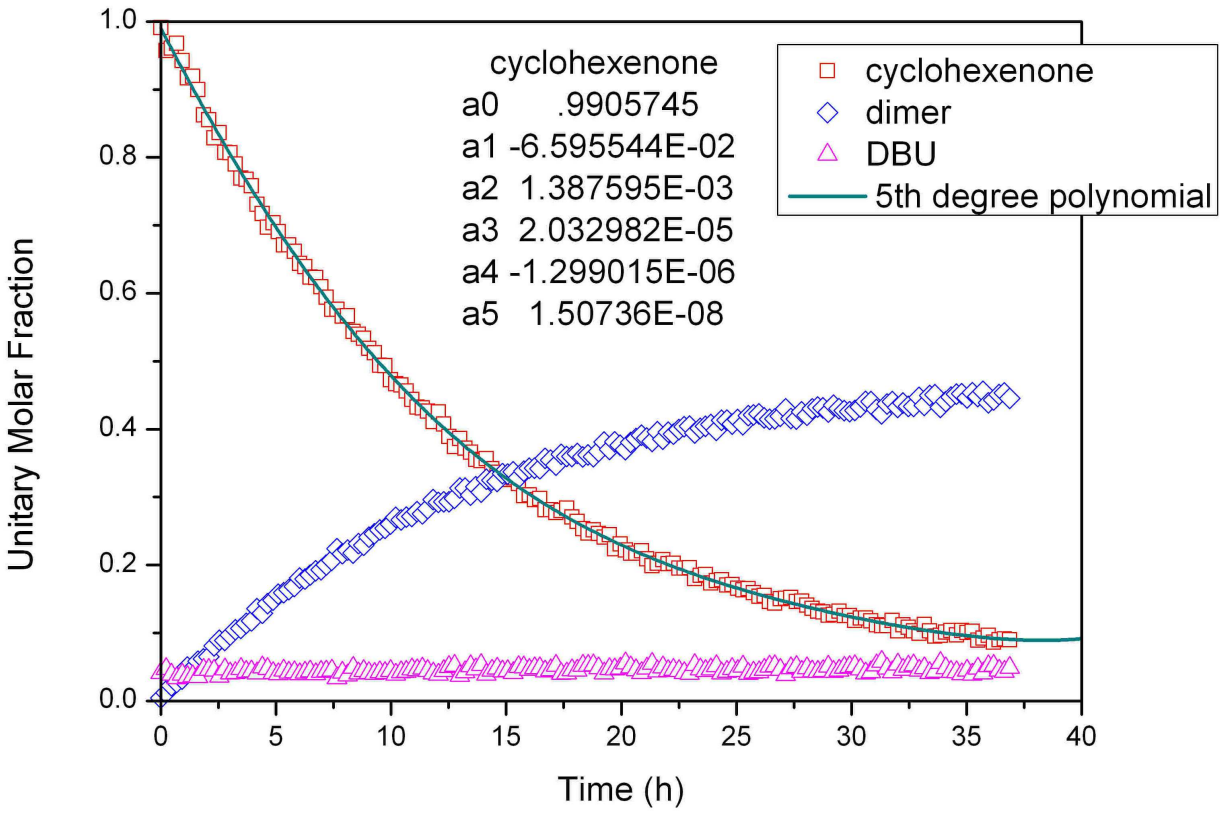

Figure S9. Conversion (entry 6 in the table) of cyclohexenone **7** into dimer **8** under the catalysis of DBU **6**. The rest of the caption as in Figure S6.

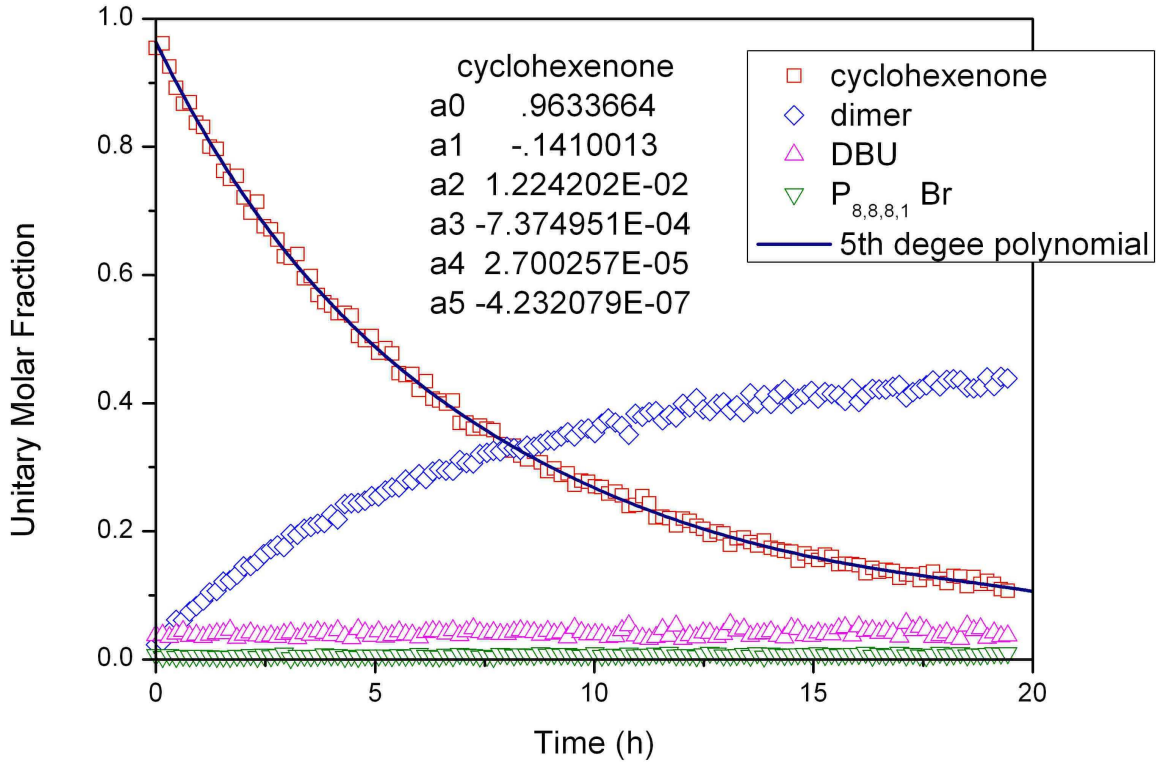

Figure S10. Conversion (entry 7 in the table) of cyclohexenone **7** into dimer **8** under the cocatalysis of $P_{8,8,8,1}$ Br **3** and DBU **6**. The rest of the caption as in Figure S6.

This journal is © The Royal Society of Chemistry 2012

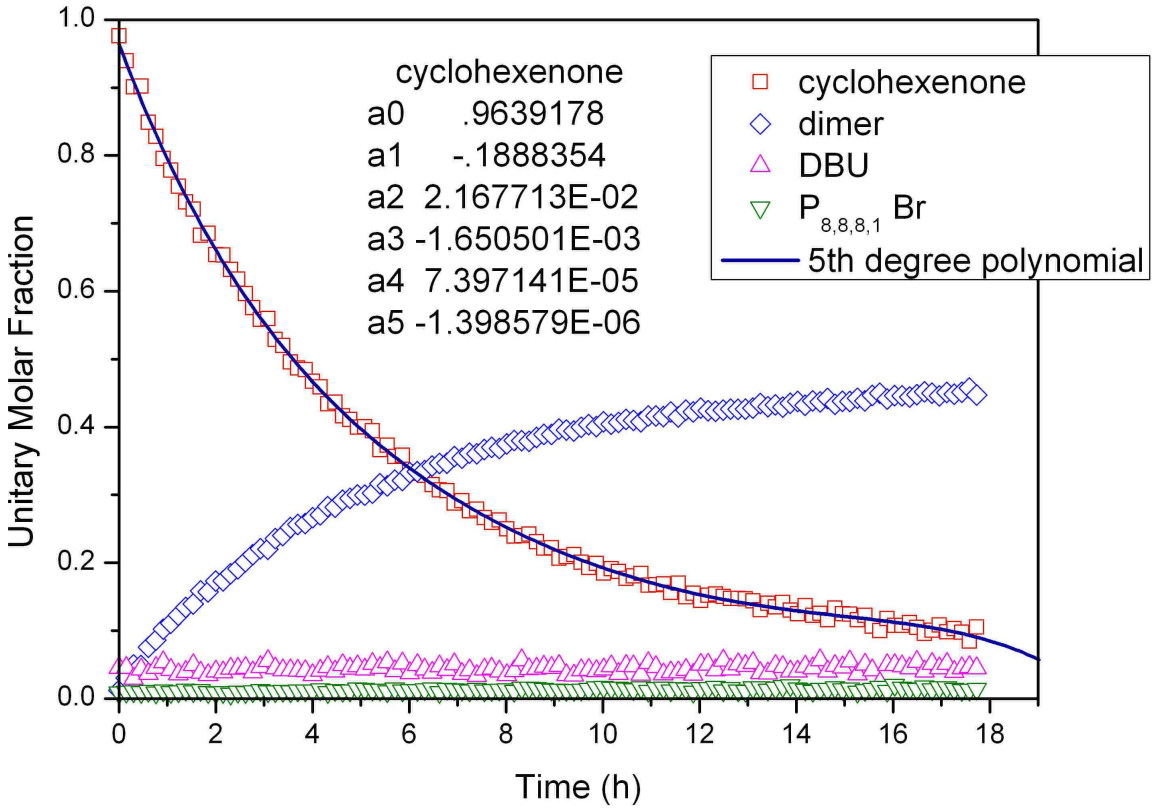

Figure S11. Conversion (entry 8 in the table) of cyclohexenone **7** into dimer **8** under the cocatalysis of $P_{8,8,8,1}$ Br **3** and DBU **6**. The rest of the caption as in Figure S6.

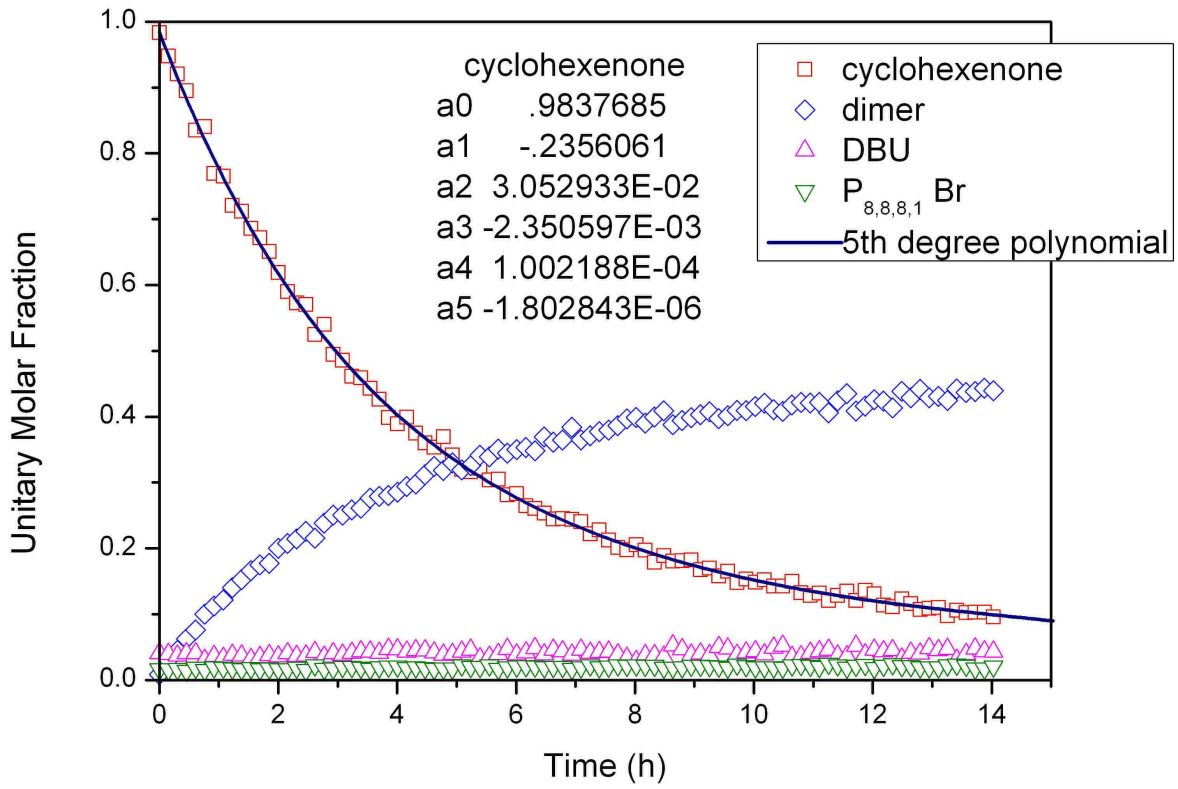

Figure S12. Conversion (entry 9 in the table) of cyclohexenone **7** into dimer **8** under the cocatalysis of $P_{8,8,8,1}$ Br **3** and DBU **6**. The rest of the caption as in Figure S6.

This journal is © The Royal Society of Chemistry 2012

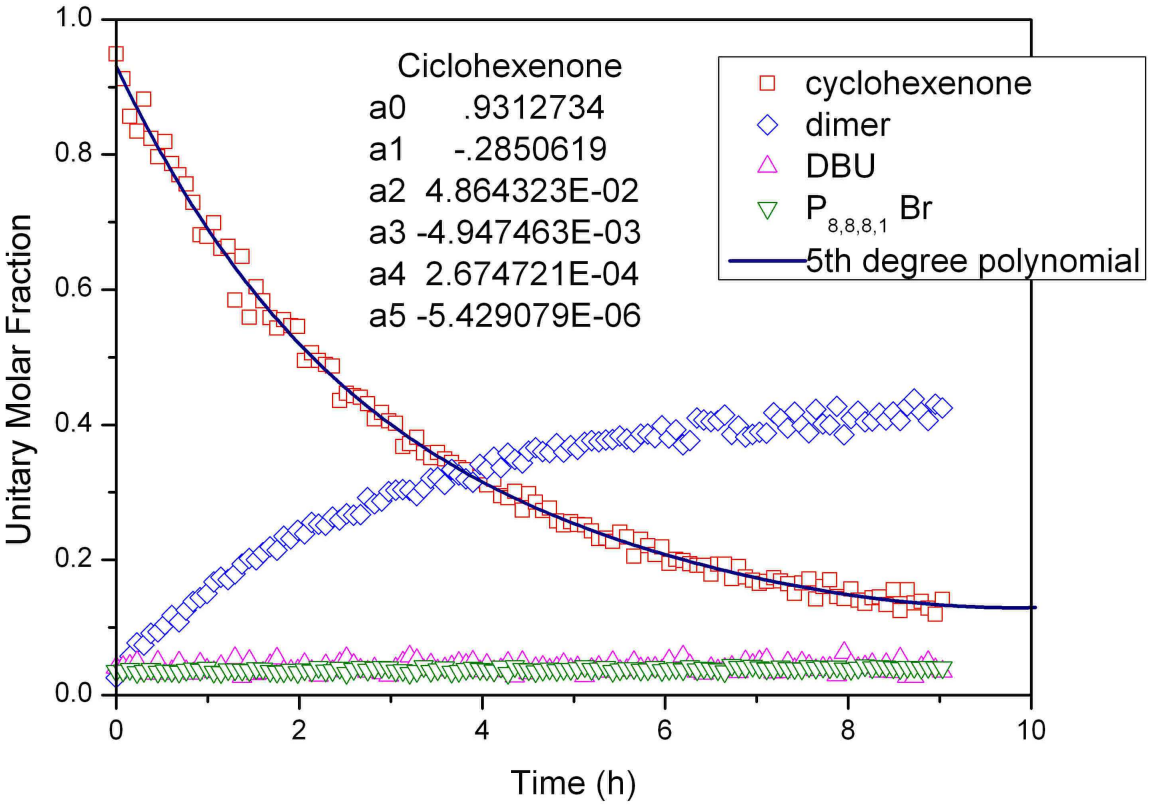

Figure S13. Conversion (entry 10 in the table) of cyclohexenone **7** into dimer **8** under the cocatalysis of $P_{8,8,8,1}$ Br **3** and DBU **6**. The rest of the caption as in Figure S6.

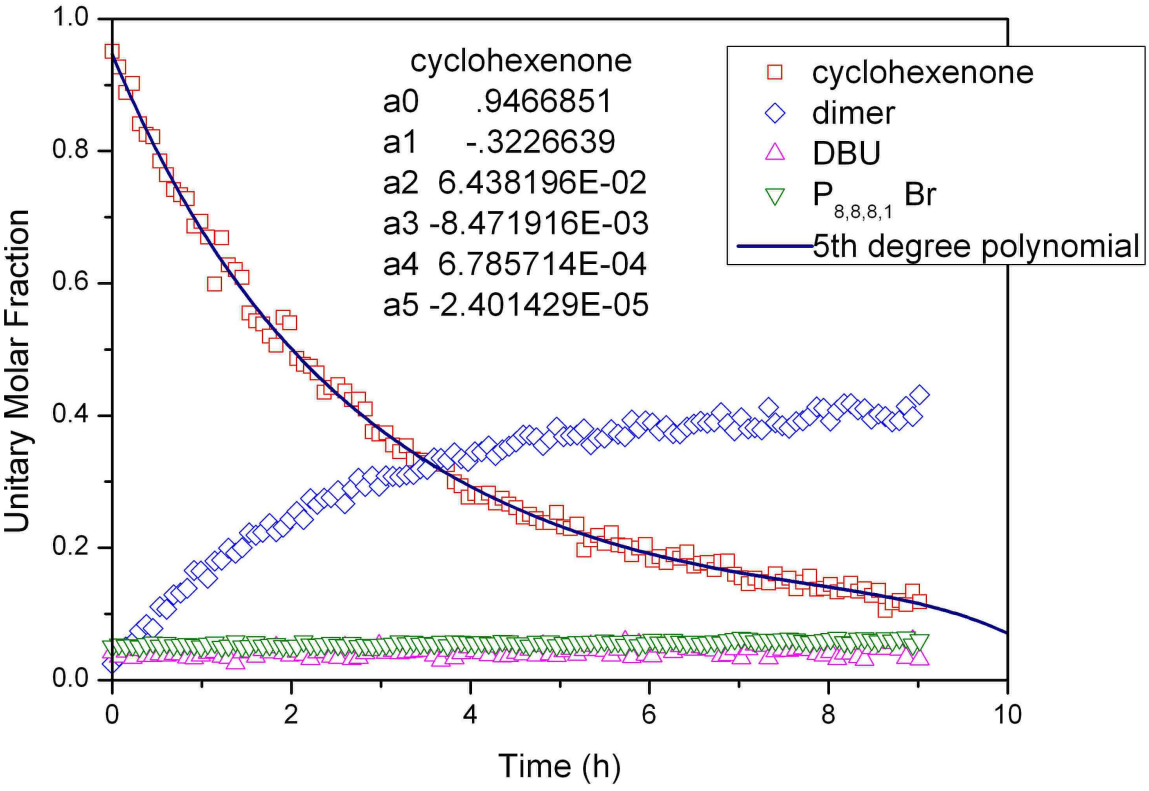

Figure S14. Conversion (entry 11 in the table) of cyclohexenone **7** into dimer **8** under the cocatalysis of $P_{8,8,8,1}$ Br **3** and DBU **6**. The rest of the caption as in Figure S6.

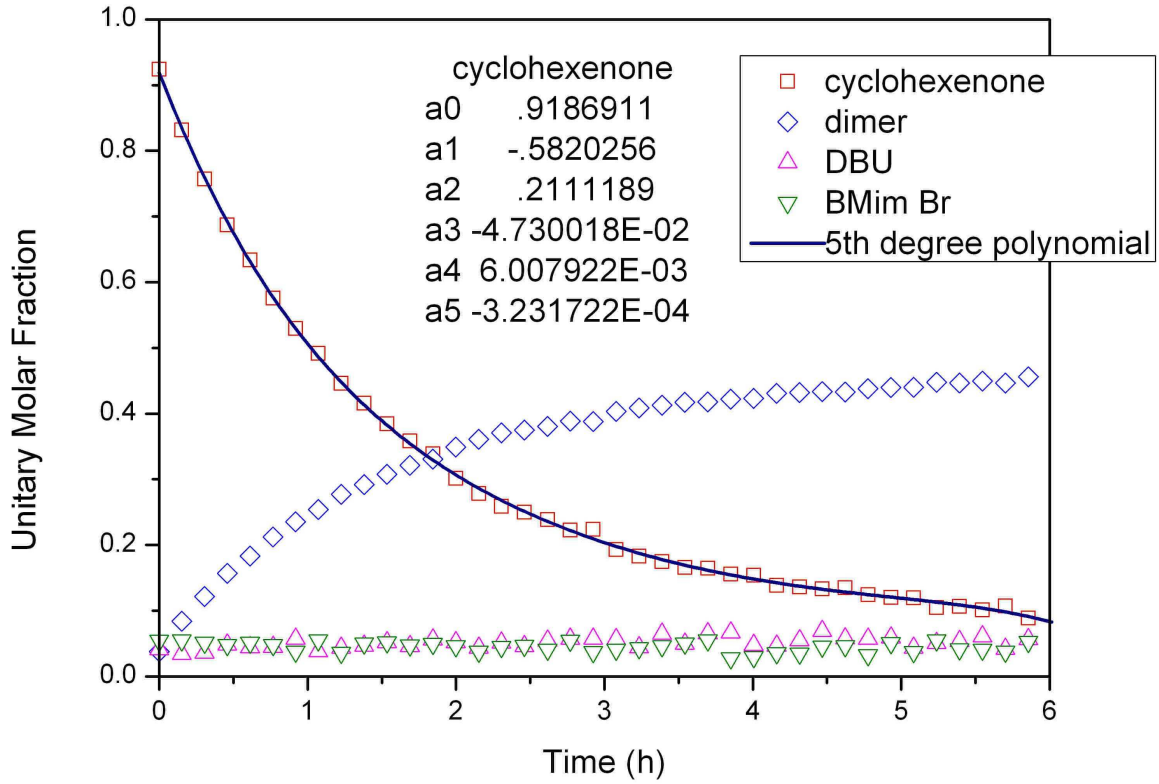

Figure S15. Conversion (entry 12 in the table) of cyclohexenone **7** into dimer **8** under the cocatalysis of BMim Br **4** and DBU **6**. The rest of the caption as in Figure S6.